AIAA 2003-0749

DEVELOPMENT OF A FREE-TO-ROLL TRANSONIC TEST CAPABILITY (Invited)

F. J. Capone, D. B. Owens, and R. M. Hall
NASA Langley Research Center
Hampton, Virginia

41st AIAA Aerospace Sciences Meeting and Exhibit

6-9 January 2003
Reno, Nevada

Development of a Free-To-Roll Transonic Test Capability

F. J. Capone†, D. B. Owens, and R. M. Hall*
NASA Langley Research Center, Hampton, Virginia

ABSTRACT

As part of the NASA/Navy Abrupt Wing Stall Program, a relatively low-cost, rapid-access wind-tunnel free-to-roll rig was developed. This rig combines the use of conventional models and test apparatuses to evaluate both transonic performance and wing-drop/rock tendencies in a single tunnel entry. A description of the test hardware as well as a description of the experimental procedures is given. The free-to-roll test rig has been used successfully to assess the static and dynamic characteristics of three different configurations--two configurations that exhibit uncommanded lateral motions, (pre-production F/A-18E and AV-8B), and one that did not (F/A-18C).

SYMBOLS AND ABBREVIATIONS

AWS	abrupt wing stall
C_A	axial force coefficient
C_{ϕ}	rolling moment coefficient
C_N	normal force coefficient
C_m	pitching moment coefficient
C_n	yawing moment coefficient
C_Y	side force coefficient
FTR	free to roll
LERX	leading edge root extension, percent
M	Mach number
t	time
δ_{te}	trailing edge flap angle, deg
ϕ	model roll angle, deg
θ	model pitch angle, deg
16-ft TT	16-Foot Transonic Tunnel

†Senior Research Engineer,
Configuration Aerodynamics Branch
§Research Engineer
*Senior Research Engineer,
Configuration Aerodynamics Branch, Member AIAA

INTRODUCTION

A joint NASA/Navy Abrupt Wing Stall Program (AWS) was established after several pre-production F/A-18E/F aircraft experienced severe wing-drop motions during the development stage. A Blue Ribbon Panel determined that a poor understanding of these phenomena existed and made the recommendation to: "Initiate a national research effort to thoroughly and systematically study the wing drop phenomena." The problem area addressed by the AWS Program[1-17] is the unexpected occurrence of highly undesirable lateral-directional motions at high-subsonic and transonic maneuvering conditions. One of the recommendations from reference 2 was to "develop a relatively low-cost, rapid-access wind-tunnel approach that combines the use of conventional models and test apparatuses to evaluate both transonic performance and wing-drop tendencies (using free-to-roll approach) in a single tunnel entry."

The overall objective of free-to-roll (FTR) testing is to identify early the potential of existence of uncommanded lateral motions. Together with the force and moment data, free-to-roll testing can: determine the severity of model motions; assess the impact of unsteady and nonlinear aerodynamics (rate and amplitude); and determine dynamic aerodynamic data (roll damping). Figure 1 shows a schematic of the free-to-roll test setup. With the model given a degree of freedom in roll, kinematic variations of angles of attack and sideslip occur during the rolling motions.

The free-to-roll test technique has been used for subsonic studies for over 30 years. For example, a research effort by NASA-Langley utilized free-to-roll testing to evaluate the F-4 wing wing-rock behavior[2, 18]. For this investigation, the model used a bearing and a dummy force balance

to provide a single degree of freedom in roll. Northrop and the Ames Research Center conducted static and semi- free-to-roll tests on a F-5A model[19] to study wing-rock motions seen in flight. For these tests, a special sting with a torsional spring and variable damper was used. NASA-Langley has used single-degree-of-freedom free-to-roll wind tunnel tests to successfully predict rolling motions at low speed and high angles of attack Low-speed testing of the X-29 forward swept wing aircraft[20] discovered wing rock before flight. This enabled changes to be made to the flight control system to handle the wing rock. Other published free-to-roll studies by Langley include an assessment of the effects of fuselage forebody geometry on stability and control[21] and wing rock characteristics of slender delta wings [22].

As part of the AWS program, pathfinder tests were conducted in the Langley Transonic Dynamics Tunnel on a 9-percent lightweight composite model of the F/A-18E (fig. 2). The objectives of this investigation were to: measure static forces and moments with a traditional force balance; conduct forced oscillation tests using a roll oscillation balance; and do a free-to-roll test without a force balance. This test used as much existing hardware as possible. The lightweight, low roll inertia model was required because of limitations of the roll oscillation balance. Some typical results from that investigation are given in figure 3. For α = 7°, the model was damped with only minor deviations in rolling motion caused by tunnel turbulence. At α = 7.5°, intermittent large-amplitude wing-drop events occurred. At α = 8°, the model exhibited large-amplitude (±40°) rolling motions. In general, FTR activity was observed in regions where severe breaks in the lift and rolling moment curves occurred.

Based on these encouraging results, a design effort was initiated to develop a free-to-roll test rig that could handle a variety of conventional wind tunnel models in a transonic tunnel. The AWS program identified three models for which free-to-roll testing was desired. These included the AV-8B, F-18C, and the preproduction F/A18E. These models had wing areas that ranged from 1.33 to 5.18 sq ft and had weights that ranged from 55 to 490 lbs. This paper will discuss the requirements imposed on the new free-to-roll rig as well as describing the hardware arrangement. In addition, the safety analysis, experimental setup and testing performed during checkout phases without a model will be discussed. Results of tests of the three configurations are presented in references 9, 10 and 14.

In order to obtain approval for releasing this paper to the public, quantitative information has been removed from most vertical scales as per guidelines from the Department of Defense.

FREE-TO-ROLL DESIGN REQUIREMENTS

A major objective of the AWS project was the desire to conduct free-to-roll testing on three different fighter aircraft configurations of varying sizes and weight as shown in figure 4. The sketches of the models are to the same scale in order to convey the relative model sizes used in the tests. Two of these configurations were known to have “wing drop” problems and the other two did not. The Langley 16-Ft. Transonic Tunnel was chosen because its large size permits testing of a wide range of model sizes.

In order to achieve this objective, the following requirements were imposed on the design of the free-to-roll rig:

- The rig had to meet all Langley safety and LAPG 1710.15 design requirements[23].
- Must be able to use existing industry high strength models for testing at higher Reynolds numbers. Thus, no separate model would need to be fabricated.
- Must be able to handle wind tunnel models of varying sizes and weights.
- The force balance was to be retained and used during testing.
- No set time required removing the force balance to install the free-to-roll rig or to test in the free-to-roll mode.

In addition, the following mechanical design requirements were also specified:

- The free-to-roll rig would replace the standard sting butt in the 16-Ft Transonic Tunnel
- The maximum normal force would be 4000 lbs.
- A high-response device was needed to measure model roll angle.
- Some means of fixing the rotating mechanism to the fixed hardware so that conventional static testing could be done.
- A mechanical hard stop with damping.
- An independent braking system.
- A counterweight to adjust the model c.g. to the axis of rotation.
- Remotely actuated fins were desired for trimming the model

FREE-TO-ROLL DESIGN

Description of Free-To-Roll Rig

The free-to-roll rig was designed to replace the standard sting butt[24] in the 16-Ft. Transonic Tunnel such that a model could freely rotate about the longitudinal axis. A sketch showing the rig installed in the wind tunnel is shown in figure 5. A cross-sectional sketch of the rig is shown in figure 6 and a solid body and assembly representation of the mechanism is presented in figure 7. Since the free-to-roll replaced the standard sting butt, its the overall length was 33.93 inches and maximum diameter was 13.47 inches.

As shown in figure 6, the rig consists of a rotary head that is supported in a stationary head by a spherical roller bearing, and an aft needle bearing. This arrangement allows thermal expansion and some shaft flexibility without binding on the bearings and also allows significant loading capability in excess of current requirements. The spherical bearing has a load rating of 102,000 lbs and the needle bearing has a load rating of 15,600 lbs. The rotary head is held onto the stationary head with a large carbon steel draw nut at the forward face of the stationary head.

The initial design of the free-to-roll rig called for dampened hard stops to be located at ±40°, ±60°, and ±80° rotation from the top center as shown in figure 7. However, during the fabrication, this was changed to a single stop located at the top center location as shown in figure 6. In addition, a locking bar was provided to fix the rotating head to the stationary head when static testing was required.

The independent braking system consisted of four 24 VDC electric brakes. As shown in figures 6 and 7, the brakes are mounted in the space between the stationary and rotary heads. The brakes are mounted to the draw nut via pin posts much like brake calipers on automotive disc brakes. The brakes apply pressure to a wear plate mounted on the back of the rotary head. Brake pressure is applied by increasing current to the electromagnets inside the brakes. This design is not only streamlined, but also allows the capability to provide a soft stop to the rotary head.

Four actuated fins are provided for use in trimming the model in roll. The fins were each mounted in a pivot block that contained the fin bearings, gearing and actuator. Each fin was powered by a harmonic drive electric motor with a feedback encoder for fin position. Each fin can be actuated independently or in unison.

An adjustable counterweight assembly as shown in figure 6 can be used to balance the model to ensure that the model's vertical center of gravity location is on the centerline of the support mechanism. The assembly consisted of a vertical rod attached to which varying weights can be secured to reach the desired result.

A roll resolver was used to measure roll angle. A 5:1 mechanical gear ratio amplifies the roll angle measurement. This roll resolver has a tracking rate of 30 deg/sec.

Auto Braking System

Initially, control of the brakes was to be accomplished with the use of a simple on/off toggle switch. However, concerns were raised that very high torque loads would be imposed from applying the brakes during a sudden stop. While there was no indication that the brakes would grab when applied--that is, result in larger than expected braking torque for a given current level--this risk could probably be mitigated by "ramping up" the current provided to the brakes. In order to achieve this mode of operation, a computer-controlled auto braking system was designed.

For a symmetric model, the rolling moment is expected to be a zero under operational conditions with no sideslip. However, experience has shown that large asymmetries in rolling moments can occur under abrupt wing stall conditions. For a very large model such as the AV-8B, these asymmetries can be as high as 150 ft-lbs of torque and are indicative of the type of forcing functions present. However, under free-to-roll conditions, the total rolling moment to be braked by the system model is determined by the combined inertia and aerodynamic rolling-moments. For the design of the braking control system, the nominal dynamic stopping torque was assumed to be 140 ft-lbs (at 5 rad/sec velocity) and the maximum peak torque was 260 ft-lbs.

Brake Control System. The brake control system was designed to both deploy the brakes at a specific roll angle and then hold the model at some position in presence of a rolling torque. Hence an appropriate algorithm for braking is necessary. Initially, the brakes are deployed at a nominal braking current of 54-percent when some predetermined roll angle is reached and then the brake current is ramped up to a full 100-percent. The brake control law is only dependent on measured roll angle ϕ, and does not account for

roll rate changes that can occur when the model is exposed to unanticipated roll accelerations from unsteady flow conditions at high angles of attack.

A schematic of the computer control used is shown figure 8. A PC computer is used for implementing the control law. This system

- Provides 28V 400 Hz drive to the roll resolver
- Accepts the resolver signal conditioning instrument on an ISA bus
- Analyzes roll angle and roll rate data continuously
- Estimates the braking current required for the given roll conditions
- Drives the brakes through the power amplifier
- Provides a throughput of above 30-40Hz closed loop for braking current

The response time of the brake is a function of the gaps, the coil inductance and its resistance. From available data, the time constant is expected to be about 10-millisecond. This dictates that the bandwidth of the power amplifier driving the coils must be at least 0-100 Hz. Hence the choice of an amplifier is a linear power amplifier and not a switching mode amplifier. A four quadrant linear power amplifier with a 0-100 Hz bandwidth that can provide a current of 2 amps peak was chosen for the brake coil drive.

Model roll angle is determined with a roll resolver with an accuracy of 7 minutes (gear ratio not accounted for). A "resolver card" in the brake computer determines the final accuracy. This "resolver card" provides this excitation voltage as well as reading the roll angle signal. The overall accuracy when combining the accuracy of the resolver card, the resolver, and the 5:1 gear ratio is 4 arc minutes or 0.067 degrees. The resolver card was a custom made piece because we had to handle the resolver shaft rotating at up to 5000 deg/sec. The resolver itself has no speed limitation only the resolver card in the brake computer. Roll angle can be resolved to 0.067 degrees at FTR rig rates up to 1000 deg/sec. Since the amount of angle estimation on the resolver signal conditioner is high, a digital signal processor based PC computer ISA bus compatible instrument will be required. A gear ratio of five exists between the resolver roll angle and model roll angle.

Control Interface. The computer program was written with a graphics mode screen, which shows the system schematic (fig. 9). The graphic displayed on the computer screen represents an animated picture of the status of the free-to-roll rig that shows the roll attitude of the model in real time with an update rate of higher than 30 frames/sec, which is acceptable from a persistence of vision point of view. The display also shows the various other elements of the system such as the raw resolver angle, brake current percent, and the status of mode control. The control shows three modes of operation:

Auto mode: In this mode, the model angle ϕ is compared with the set ϕ_1, ϕ_2 and based on the control logic; a current is imposed on the brakes as per control law.

Manual Mode: Once on manual mode, there are two choices available, the *brake-off* mode or the *brake-on* mode.

Pulse mode: The pulse mode works while on Manual mode and, in the Automode only when the brakes are *ON*. The pulse mode, momentarily switches the brakes *ON* or *OFF*, to a state opposite of existing state.

Reliability and Safety Issues. From the onset of the design of the computer-controlled braking system, the central issue for the Free-To-Roll rig was reliable, accurate and quick determination of the model angle, and then when necessary, impose the desired brake current based on the prescribed control law. With the following precautions, the reliability of the logic part of the system was high and was only dependent on the quality of brake and its response

- A dedicated resolver should be used for the brake system. Sharing resolver signals with other data devices would have created issues of reliability. However, this did not turn out to be a practical solution and in the end, signal sharing was used.
- The excitation to the resolver was internally generated by the computer and hence provides high reliability as long as computer was *ON*
- The computer program was a single task program and can run as long as computer has power.
- The brake amplifier was an industrial class linear amplifier with known reliability.
- The brake power supply was an industrial class switching mode device with high reliability.
- The computer power and brake power was provided from an uninterrupted supply at the 16-Ft Transonic Tunnel.
- Protected wiring from resolver, to the brake power system was provided.
- The computer was prevented from inadvertent reset by locking the power *ON*. Provision for keyboard lock was also desirable.

SAFETY ANALYSIS

Required Safety Analysis

All models tested in various wind tunnels at the Langley Research Center must adhere to the strict requirements set forth in reference 23. This guide contains criteria for the design, analysis, quality assurance and documentation of wind-tunnel model systems to be tested. A wind-tunnel model system includes model support hardware including force balances and stings. A Model Systems Engineer serves as the resident expert for the review of the model systems design and analysis. His findings are reported to the Facility Safety Head who is the final approval authority for all models to be tested in the facility. Since these requirements are incorporated in the overall Langley Safety manual, further reviews by a safety engineer may be required, which was the case for the free-to-roll rig.

All the parts of the free-to-roll rig met the required safety factors of 4 on ultimate and 3 on yield. Both the stationary head and rotating head were analyzed using hand calculations and finite element analysis.

All model systems are designed for a system failure event, that is, the design shall be such that after an initial failure, the model shall not experience any further failure that would cause facility damage during the tunnel shutdown process. Under this requirement, a failure of the independent braking system was not considered a safety issue, since any rotation of the model would be halted with the mechanical hard stop. A concern was raised concerning impact loading on the force balance and an attempt was made to remove it. However, in the absence of any analysis, the safety engineer wanted the hard stop to be retained even though having the model essentially spinning was not considered a safety issue.

It should be noted, that additional stress analyses are required for the wind-tunnel model itself to account for inertial loads that would be imparted to key model components due to high accelerations in roll if the model is experiencing wing drop or rock.

Brake Analysis

The braking analysis performed to assure that the brakes could arrest the model assumed (1) a worst-case forcing function, (2) took into account that the braking effectiveness was a function of time, and (3) integrated the resulting equation of motion about the body axis to predict a final bank angle, ϕ, at which the model would have come to rest.

The first task was to assume a very conservative forcing function that would model the acceleration the model might experience when it was in a wing-drop region. The basis for this assumption was data from the proof-of-concept experiment in the TDT. The data are illustrated in figure 10 and relate the roll acceleration of the model, $d^2\phi/dt^2$, as a function of ϕ. For analysis purposes, it is assumed that the model only experiences an aerodynamic propelling function for $-20° < \phi < 20°$. The forcing function in the data of figure 10 is seen to act between 8° and 30° of ϕ and spikes to a value of 2500 deg/sec^2 for $d^2\phi/dt^2$. To be on the conservative side, the notional forcing function for the analysis was assumed to occur over a range of bank angles between 0° and approximately 45° and to be of a magnitude of between 4300 and 4900 deg/sec^2, depending on Mach number. This region is approximated by the dotted line in figure 10 and illustrates the extremely conservative characterization for the forcing function.

The second task was to characterize the brake effectiveness as a function of time. The first model was assumed to be a ramp function, where at some preset bank angle, ϕ, the brakes would instantly have 50% of the assumed maximum braking power. This power would then linearly ramp up until it reached 100% of assumed maximum braking power. A second model was later employed when it was realized that the brakes took a finite time to energize as the coil was charged. Both models are graphically described in figure 11.

Results for both braking models are illustrated in figure 12. The top two figures are for the coil brake effectiveness model. The model being used for this example was the AV-8B. With the assumed forcing function of 4300 deg/sec^2, the model can achieve a roll rate of 120 deg/sec before the forcing function ceases near ϕ = 45º. With the brakes being actuated at ϕ = 50º, the calculation predicts a value of ϕ for model at rest of just over 160°. Using the ramp-braking model predicts a lower stopping rotation of less than 140°.

These calculations, which assumed ideal brake effectiveness, were not intended to be precise predictions of what would happen during the experiment. They were intended to be engineering estimates that would show that the brakes could safely arrest the model before it

would reach bank angles beyond 180°, which held true during the experiments.

One result indicated by the brake analysis was that if a model was halted by the mechanical hard stop, the impact load was such as to overload the roll component on the force balance. In addition, there was some question how to analyze the loads imparted to the model due to a sudden acceleration. With this new information, a new assessment of the hard stop was made and a decision was reached to remove it. The only risk identified to a model spinning would be twisting of the various instrumentation leads with a possibility of the leads breaking. This also was not considered a safety issue.

Risk Analysis

Both NASA and NAVAIR personnel not associated with the required analysis previously discussed made an independent risk assessment. The initial assessment, shown in figure 13, indicated three high and three medium risk items present. It is very unlikely that a Facility Safety Head would allow any testing to occur with any item identified as a high risk. After careful considerations, all the high and medium risk items were downgraded to a low risk status.

The first item was eliminated with the decision to remove the hard stop. The second item was downgraded because of the extra stress analysis required to account for inertial loads. In addition, roll loadings are continuously monitored during testing by safety systems in the 16FTT. If any load or combination of loads exceeds 100% of balance/model limits, testing is automatically terminated at that condition. The third and sixth risks were addressed by conducting a ground vibration test rap assessment before FTR testing for each of the 4 configurations. Frequencies were monitored during testing to ensure that no coalescing would take place. Again, there is in place at the 16FTT, a safety system that had the capability to not only monitor these various frequencies, but also to automatically reduce tunnel speed in the event of an occurrence. A very stringent analysis is already performed on any model support system as part of the required safety analysis. There little likelihood of overstressing either the FTR rig or sting because of the safety monitoring systems used. The fifth risk was eliminated because of the installation of the automatic braking system. Figure 14 shows the resulting risk assessment after the risk mitigations.

SYSTEM CHECKOUT

Extensive pretest testing of the free-to-roll rig was performed in the model build up bay at the 16-Ft. Transonic Tunnel without a model mounted to the rig. Functional tests of the fin actuation system, brakes and the automatic braking system were performed. Sting bending characteristics of the rig with the locking bar attached were done and these results were compared to those measured previously with the sting mounted to the standard sting butt. One very important part of these tests was to help in developing test techniques and to give the operators training in the use of the rig.

During this time, it was found that the brakes did not completely disengage when the current to the brakes was turned off. As a result, sets of external springs were installed to pull the brakes back when they were not actuated.

In addition, system friction characteristics were measured wind-off, and wind-on fin tares were determined. Measurements were made to determine the friction from the bearings and any residual brake contact with the rotor. It is essential to know the magnitude of the friction moment since this moment can be a source of error when determining the roll damping for the various models. Friction is determined by using the roll angle time history resulting from a release of the counter weight from an initial angular displacement. Ideally, one would want to load the rig to those exhibited by the model in the wind tunnel. However, no *safe* way was been determined to measure the friction with the bearings loaded at the wind-on forces generated by the models.

Estimates of rolling friction from the FTR rig were made by pendulum tests with no model prior to testing. Additional estimates were made during wind tunnel tests with another model by measuring the rolling moments from an internally mounted balance, and comparing those outputs with the calculated rolling moments based on roll acceleration of the model. These estimates showed some variation of friction between runs, and some differences with loads on the rig. The estimates across the range of conditions evaluated resulted in friction factor ranging from approximately μ = 0.25 to 0.65 ft-lb/rad/sec.

A wind-on fin checkout was conducted to determine roll control effectiveness from the fins and to ascertain if any uncommanded fin behavior such as fin movement when no control inputs are made or fin “buzz” was present.

Since aerodynamic moments generated by fins represent a source of error, an assessment of this error was made. With the rig and counterweight alone on the strut, the rig was displaced to some initial roll angle and held in position by the brake. After the brakes are released, the roll angle time history of the resulting motion is analyzed to determine the rolling moment generated by the fins. This was repeated at various Mach numbers, sting angles and fin deflection angles.

There were two major findings of these tests: 1.) The damping from the fins was large and increased with Mach number; and 2.) During some of these damping runs, the fins would sometimes go in the wrong direction or not damp out in a sinusoidal fashion, i.e. a meandering or the decelerations were not smooth. As a result of these finding, it was decided to remove the fins from the free-to-roll rig and proceed to testing the three models.

EXPERIMENTAL PROCEDURES

Static Force Testing. A block diagram of the experimental setup is presented in figure 15. The unfiltered signals from the force balance and other model instrumentation are sent to the wind tunnel data acquisition system (NEFF), an analog amplifier-conditioning unit (analog-to-digital converters). The NEFF filters and amplifies the analog signal and passes it on to the wind tunnel computer (ModComp).

This NEFF unit also sends unfiltered and buffered signals on to other devices such as the RMS converters, the Balance Dynamic Display Unit (BDDU) and the Model Protection Safety System (MPSS). The RMS converters generate a DC signal representing a RMS value of the unfiltered signal that is sent back to the NEFF. The NEFF then filters and amplifies the signal and sends the filtered signal to the Modcomp. The filtered signals are then recorded by the ModComp depending on the mode operation.

The BDDU normalizes and multiplexes the unfiltered and buffered signals from the NEFF so that the displayed output on an oscilloscope denotes percent of full-scale design loads in six sequential horizontal locations. Two-level visual and audible alarms are incorporated to indicate when a signal exceeds 70% and 100% of the static plus dynamic design load. This system requires some predetermined operator action when 100% design load is reached.

The Model Protection Safety System (MPSS) monitors corrected balance component inputs to identify excessive loads on the balance, model or sting. This system gives a continuous display in percent of the static plus dynamic design loads. The MPSS allows for a number of configurable load limits including combinations of the forces and moments. If one of the limits are exceeded or the balance voltage is out of tolerance the MPSS sounds an audible alarm and begins driving the tunnel fan speed down to reduce the tunnel dynamic pressure

Free-To-Roll Testing. During free-to roll testing, all of the systems just described are also used. Since free-to-roll testing is inherently time history in nature, the free-to-roll testing requires three additional forms of "data" acquisition. One form is the videotaping of the rolling motions of the model. Overlays on the video of tunnel conditions, run numbers, etc. and a flag of when roll angle time histories are being acquired by the data acquisition make post processing and syncing of the video to roll angle time histories possible. The second form is the digitizing of the roll angle signal. A computer in the control room where the engineer can quickly analyze the signal for frequency, amplitude, roll rates, and roll accelerations content processes this signal immediately. This information is then fed to the final form of "data" acquisition. This final form of data acquisition is written "pilot" comments in the form of a run log. These comments can be verbally recorded on the videotape as well. This written run log allows a quick assessment of the nature of the rolling motions during the free-to-roll phase.

Modes of Operation. There are two modes of operation with the free-to-roll rig. First, conventional static testing is accomplished by having the locking bar in place. The signals from the NEFF are passed through 1 Hz filters and data is then recorded for 5 seconds at 10 frames/second. Model roll angle in this mode is determined from the standard instrumentation located within the model strut support system. Testing in the static mode is then conducted using the standard procedures in place at the 16-Ft. Transonic Tunnel.

For free-to-roll testing, the locking bar is removed. Prior to starting the wind tunnel, the brakes are deployed with the model at roll angle of 0°. In this mode, the signals from the NEFF are passed through 10 Hz filters and data is then recorded continuously at 100 frames/second. Model roll angle is determined from the roll resolver. Three separate test techniques are employed during FTR testing. First the model is pitched continuously from some low pitch angle to the maximum angle desired. Next, a series of

pitch-pause tests are conducted. With the brakes set, the model is pitched to the desired pitch angle and then the brakes are released. For the third technique, the model is displaced to some initial roll angle and held in position by the brake. After the brakes are released, the roll angle time history of the resulting motion is analyzed to determine the roll damping characteristics of the model. Further details of these techniques as well as results of the tests conducted on the three wind tunnel models can be found in references 10 and 14.

One of the major requirements in the design of the free-to-roll rig was the force balance was to be retained and used during testing. There were risks involved with this requirement but it was felt that the having the force balance would prove to be invaluable in particular from a safety standpoint in being able to monitor model loads during FTR testing. The risk posed by damage to the balance has been discussed previously. There was always a concern that the forces and moments measured during free-to-roll testing would be erroneous. However, this turned out not to be the case. Comparisons were made of the measured forces and moments between FTR and static testing for different cases when a model did or did not exhibit any free-to-roll activity. Although not shown, excellent agreement was found to exist for the longitudinal data for the two test modes. A further discussion of these results can be found in reference 14.

ACCOMPLISHMENTS

A new free-to-roll test rig has been designed and built for transonic testing. This is a national test asset that can be used to determine potential uncommanded lateral motions early in the design stage. The free-to-roll test rig has been used successfully to assess the static and dynamic characteristics of three different configurations (fig. 16).

During these tests, the safety procedures, general test approach and interpretation of results have been very successful.

ACKNOWLEDGEMENTS

The authors would like to thank Mr. Joe Chambers for motivating the use of the free-to-roll technique in the transonic speed regime. Mr. Sundareswara Balikrishna of Vigyan, Inc. designed the computer-controlled automatic braking system.

REFERENCES

1. Hall, R. M.; and Woodson, S: *Introduction to the Abrupt Wing Stall (AWS) Program*. AIAA-2003-0589, January, 2003.
2. Chambers, J. R.; and Hall, R. M.: *Historical Review of Uncommanded Lateral-Directional Motions at Transonic Speeds.* AIAA-2003-0590. January, 2003.
3. McMillin, S. N; Hall, R. M.; and Lamar, J. E.: *Understanding Abrupt Wing Stall with Experimental Methods*. AIAA-2003-0591, January, 2003.
4. Woodson, S.; Green, B; Chung, J.; Grove, D.; Parikh, P.; and Forsythe, J.: *Understanding Abrupt Wing Stall (AWS) with CFD*. AIAA-2003-0592, January, 2003.
5. Schuster, D.; and Byrd, J.: *Transonic Unsteady Aerodynamics of the F/A-18E at Conditions Promoting Abrupt Wing Stall*. AIAA-2003-0593, January, 2003.
6. Forsythe, J.; and Woodson, S.: *Unsteady CFD Calculations of Abrupt Wing Stall Using Detached- Eddy Simulation.* AIAA-2003-0594, January, 2003.
7. Parikh, P; and Chung, J.: *A Computational Study of the AWS Characteristics for Various Fighter Jets: Part I, F/A-18E & F-16C*. AIAA-2003-0746, January, 2003.
8. Chung, J.; and Parikh, P.: *A Computational Study of the Abrupt Wing Stall (AWS) Characteristics for Various Fighter Jets: Part II, AV-8B and F/A-18C*. AIAA-2003-0747, January, 2003.
9. Lamar, J. E.; Capone, F. J.; and Hall, R. M.: *AWS Figure of Merit (FOM) Developed Parameters from Static, Transonic Model Tests*. AIAA-2003-0745, January, 2003.
10. Owens, B; Capone, F. J.; Hall, R. M.; Brandon, J; and Cunningham, K: *Free-To-Roll Analysis of Abrupt Wing Stall on Military Aircraft at Transonic Speeds.* AIAA-2003-0750, January, 2003.
11. Roesch, M, and Randall, B.: *Flight Test Assessment Of Lateral Activity*. AIAA-2003-0748, January, 2003.
12. Green, B; and Ott, J.: *F/A-18C to E Wing Morphing Study for the Abrupt Wing Stall Program*. AIAA-2003-0925, January, 2003.

13. Kokolios, A.; and Cook, S.: *Use of Piloted Simulation for Evaluation of Abrupt Wing Stall Characteristics.* AIAA-2003-0924, January, 2003.
14. Capone, F. J.; Hall, R. M.; Owens, B.; Lamar, J. E.; and McMillain, S. N.: *Recommended Experimental Procedures for Evaluation of Abrupt Wing Stall Characteristics*. AIAA-2003-0922, January, 2003.
15. Woodson, S.; Green, B.; Chung, J; Grove, D.; Parikh, P; and Forsythe, J.: *Recommendations for CFD Procedures for Predicting Abrupt Wing Stall (AWS).* AIAA-2003-0923, January, 2003.
16. Cook, S.; Chambers, J.; Kokolios, A.; Niewoehner, R.; Owens, B.; and Roesch, M.: *An Integrated Approach to Assessment of Abrupt Wing Stall for Advanced Aircraft*. AIAA-2003-0926, January, 2003.
17. Hall, R. M.; Woodson, S.; and Chambers, J. R.: *Accomplishments of the AWS Program and Future Requirements*. AIAA-2003-0927, January, 2003.
18. Chambers, Joseph R.; and Anglin, Ernie L.: *Analysis of Lateral-Directional Stability Characteristics of a Twin-Jet Fighter Airplane at High Angles of Attack*. NASA TN D-5361, 1969.
19. Hwang, C.; and Pi, W.S.: "*Investigation of Steady and Fluctuating Pressures Associated With the Transonic Buffeting and Wing Rock of a One-Seventh Scale Model of the F-5A Aircraft*." NASA Contractor Report 3061, November, 1978. NOTE: Subsequently summarized, reduced, and published as: "*Some Observations on the Mechanism of Aircraft Wing Rock." AIAA Paper 78-1456, AIAA Aircraft Systems and Technology Conference*. Los Angeles, CA. August 21-23, 1978.
20. Murri, D. G.; Nguyen, L. T.; and Grafton, S. B.: Wind-Tunnel Free-Flight *Investigation of a Model of a Forward-Swept Wing Fighter Configuration.* NASA TP-2230, February 1984.
21. Nguyen, L. T.; Yip, L.; and Chambers, J. R.: *Self-Induced Wing Rock of Slender Delta Wings.* AIAA-81-1883, August 1981.
22. Brandon, J. M.; Murri, D. G.; and Nguyen, L. T.: *Experimental Study of Effects of Forebody Geometry on High Angle of Attack Static and Dynamic Stability and Control*. ICAS, 15th Congress Proceedings, vol. 1, pp 560-572. September 1986.
23. *Wind-Tunnel Model Systems Criteria*. NASA LAPG 1710.15, September 27, 2000.
24. Capone, Francis J.; Bangert, Linda S.; Asbury, Scott C.; Mills, Charles T.; and Bare, E. Ann: *The NASA Langley 16-Foot Transonic Tunnel - Historical Overview, Facility Description, Calibration, Flow Characteristics, Test Capabilities*. NASA TP-3521, 1995.

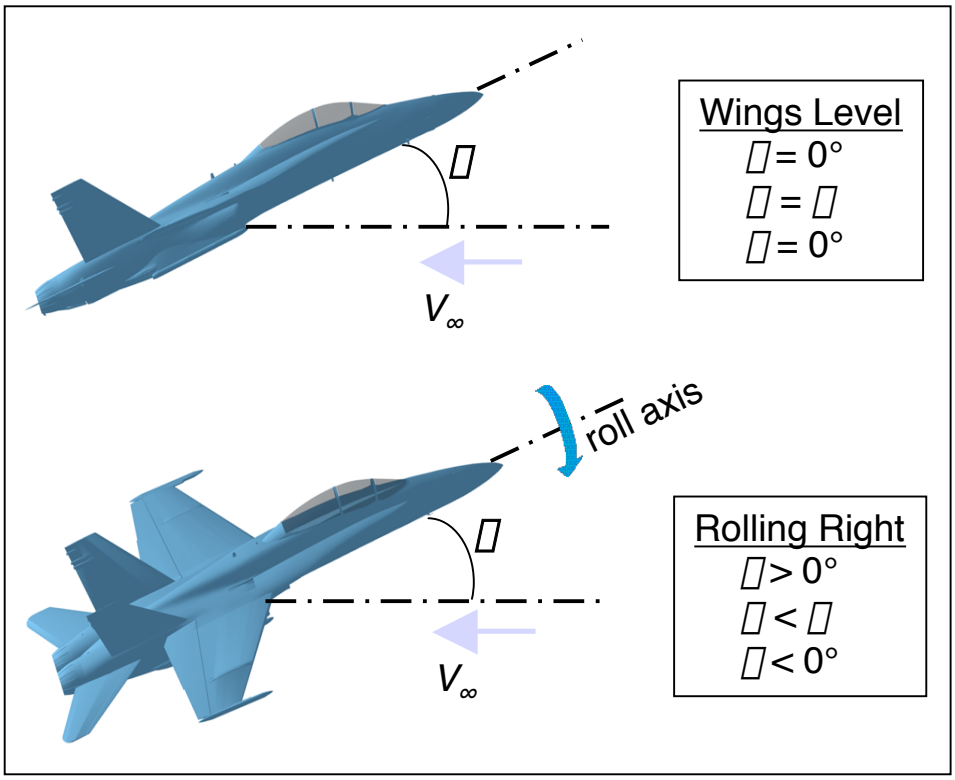

Figure 1. Notional sketch of the free-to-roll test technique.

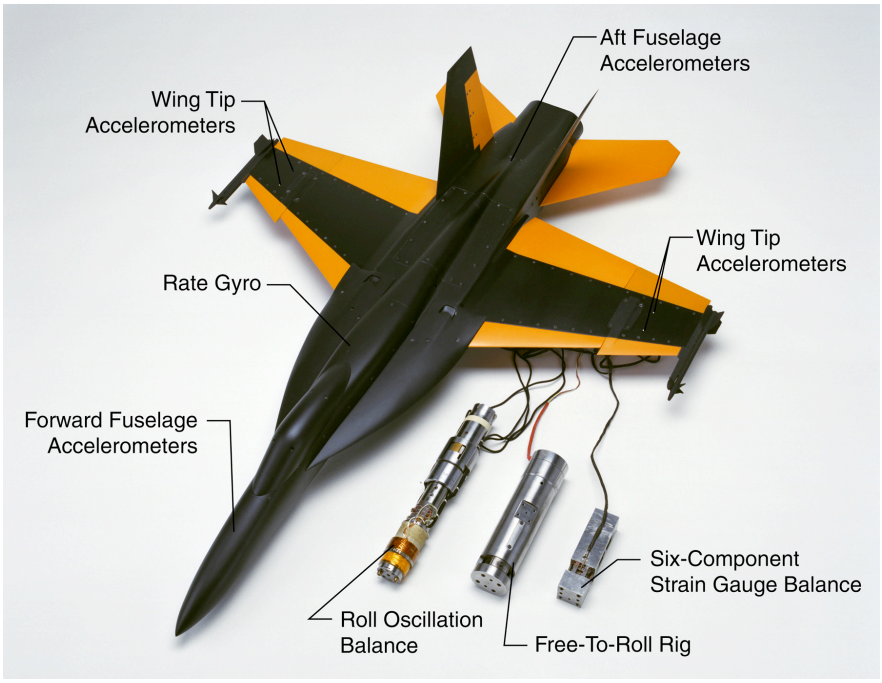

Figure 2. Photograph of the pre-production F/A-18E model Tested In the Langley Transonic Dynamics Tunnel.

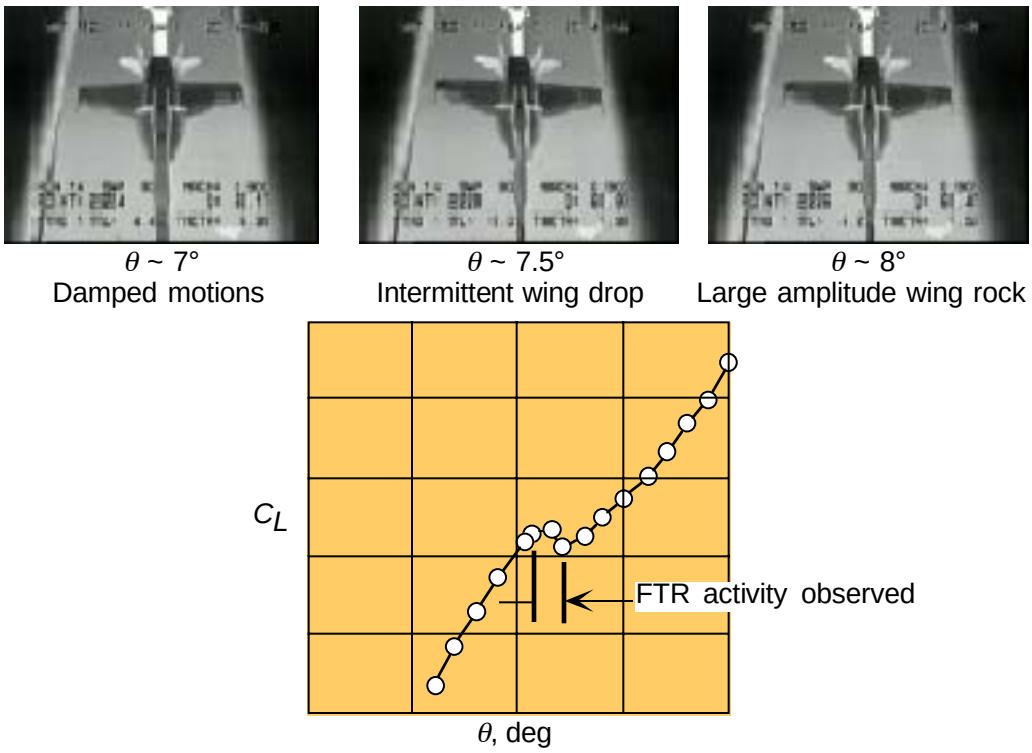

Figure 3. Typical test results from the Transonic Dynamics Tunnel.

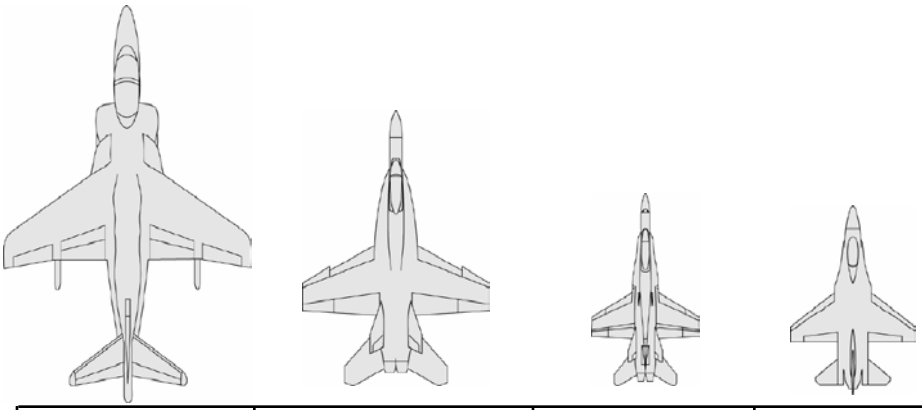

	AV-8B	F-18E/F	F-18C	F-16C
Length, in.	81.27	54.99	39.18	37.25
Wing Area, ft^2	5.18	3.2	1.33	1.67
Span, ft	4.55	3.34	2.25	2.07
Weight, lbs	490	185	55	56
Inertia, slugs-ft^2	4.0	1.2	0.2	0.2
Scale, %	15	8	6	6.67

Figure 4. Geometric characteristics of the four models tested.

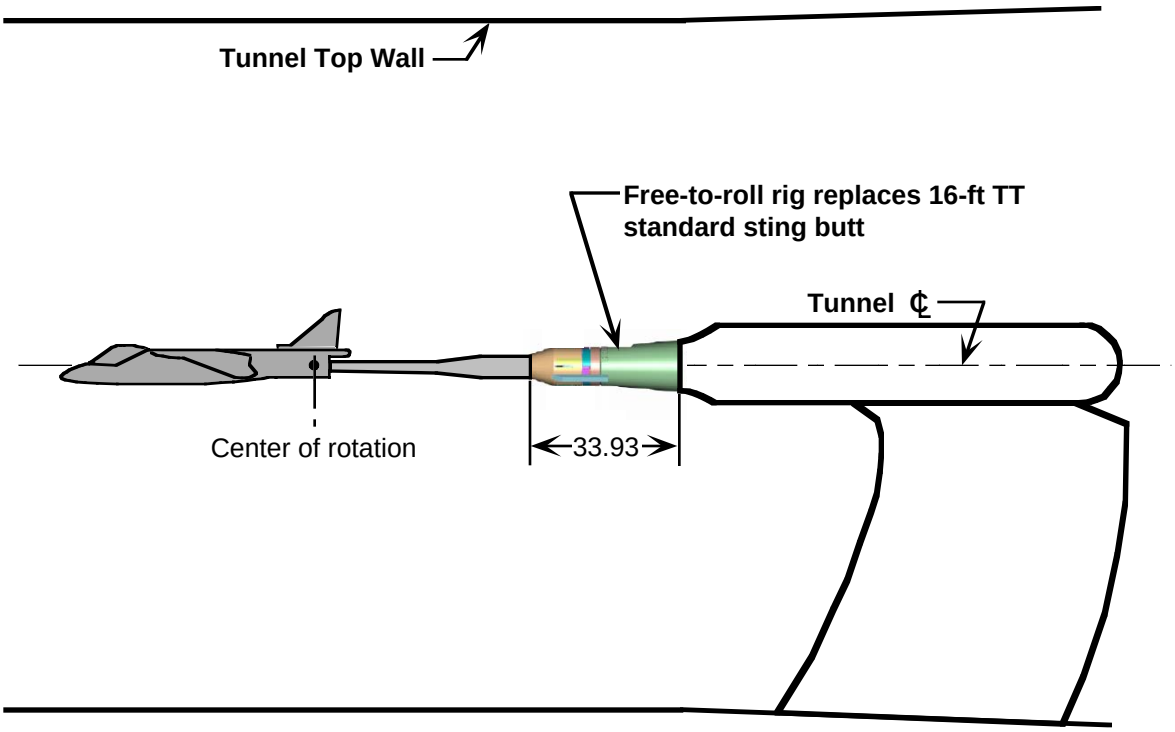

Figure 5. Sketch of free-to-roll rig installed in Langley 16-Foot Transonic Tunnel.

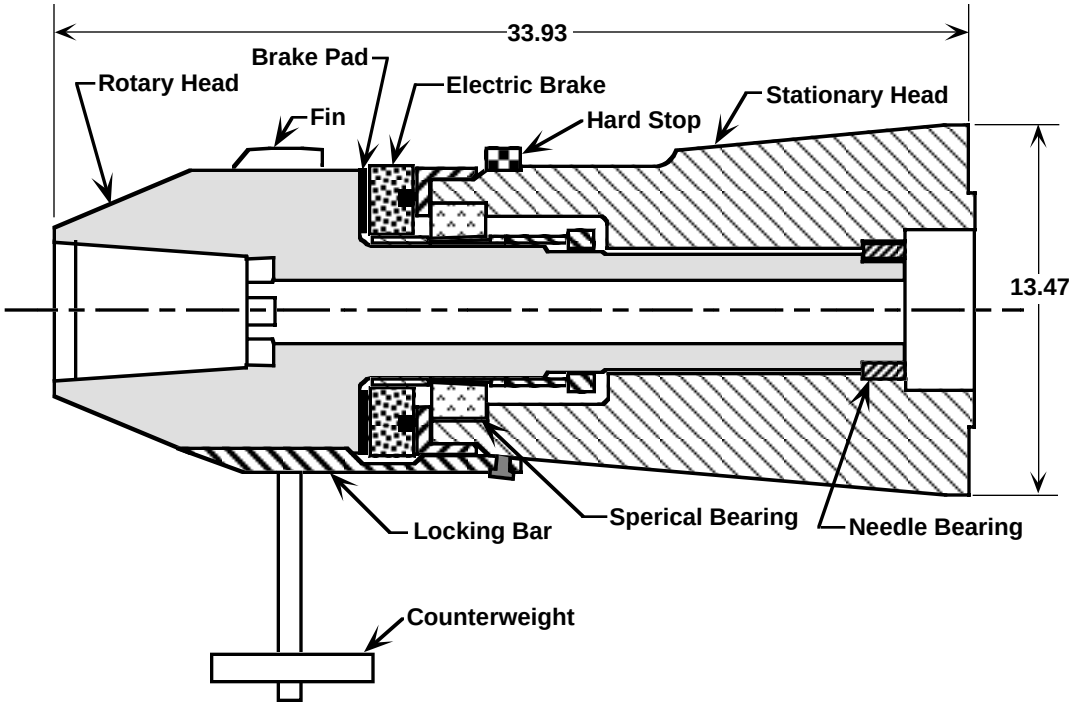

Figure 6. Cross-sectional sketch of the free-to-roll rig.

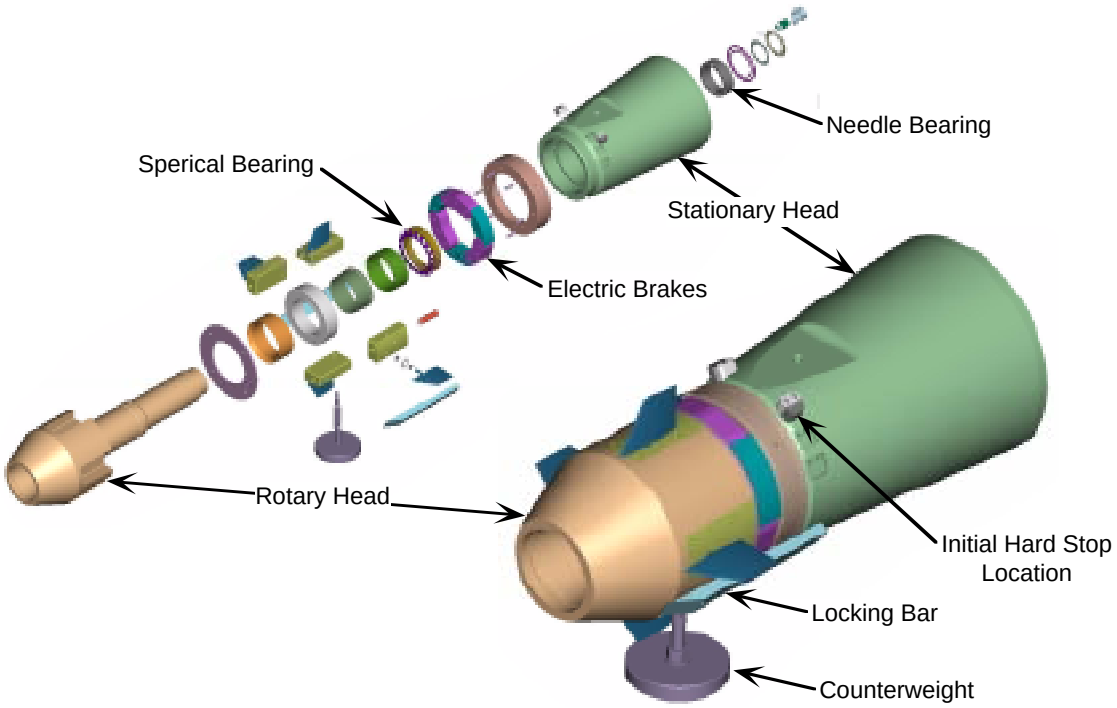

Figure 7. Solid body representative of the free-to-roll rig.

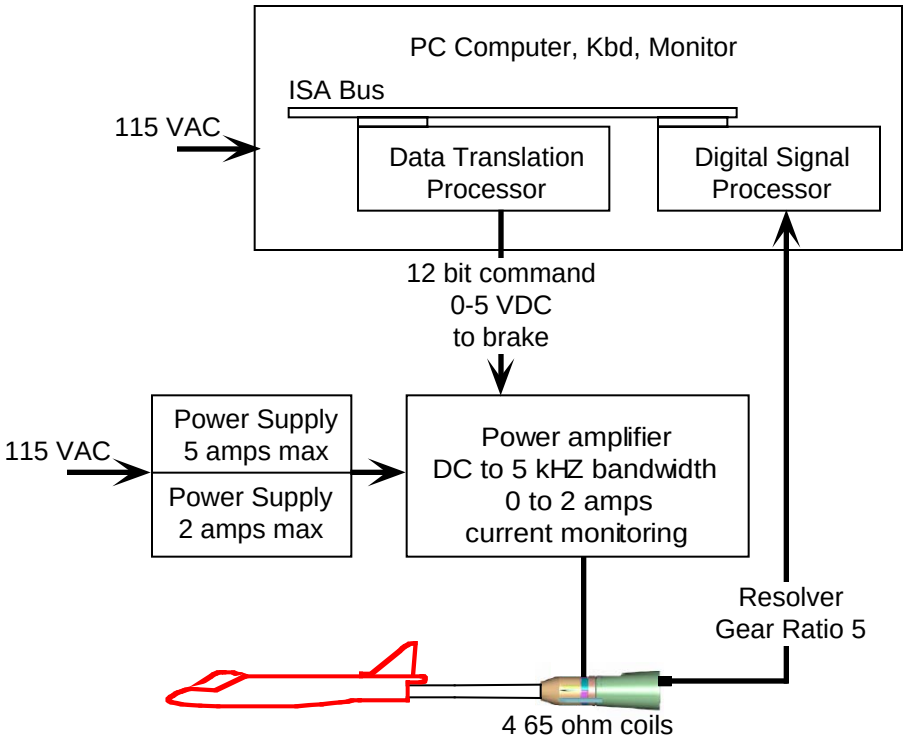

Figure 8. Schematic of computer-controlled automatic braking system.

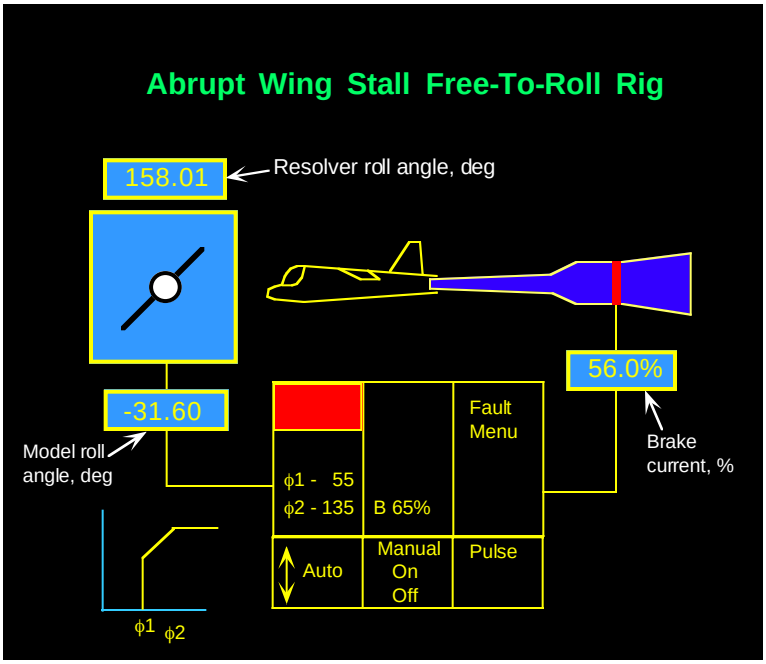

Figure 9. Braking system display monitor.

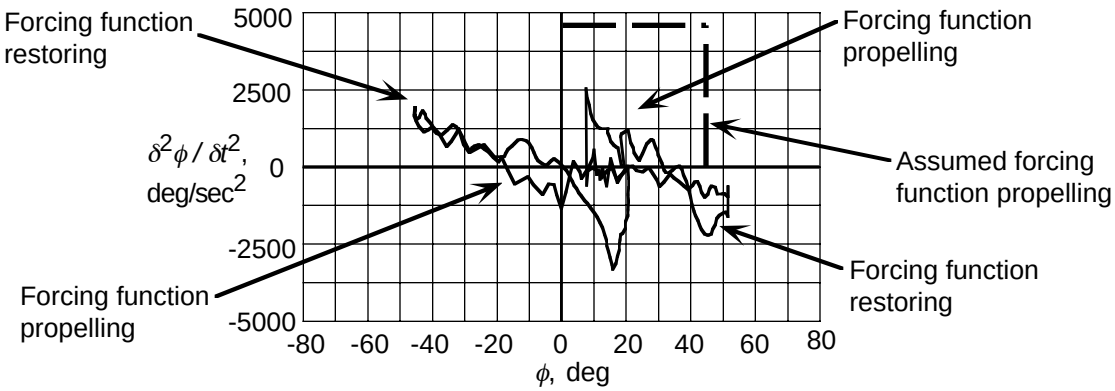

Figure 10. Typical forcing function for brake-stopping analysis.

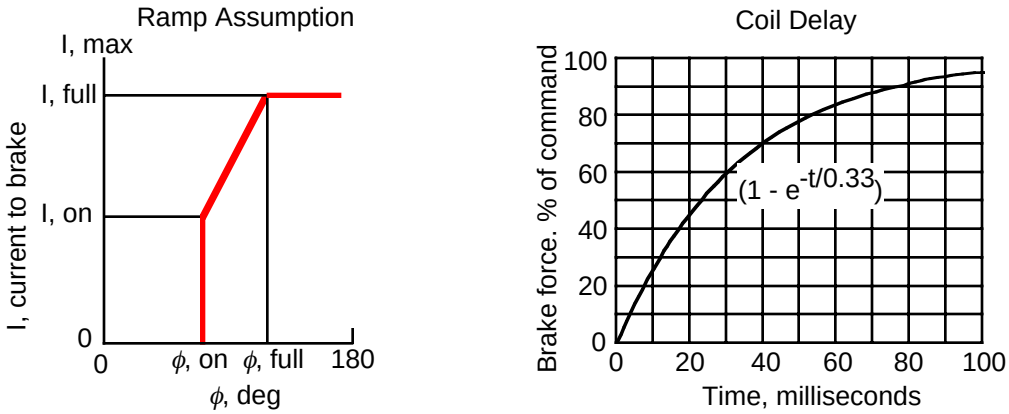

Figure 11. Brake effectiveness as a function of time.

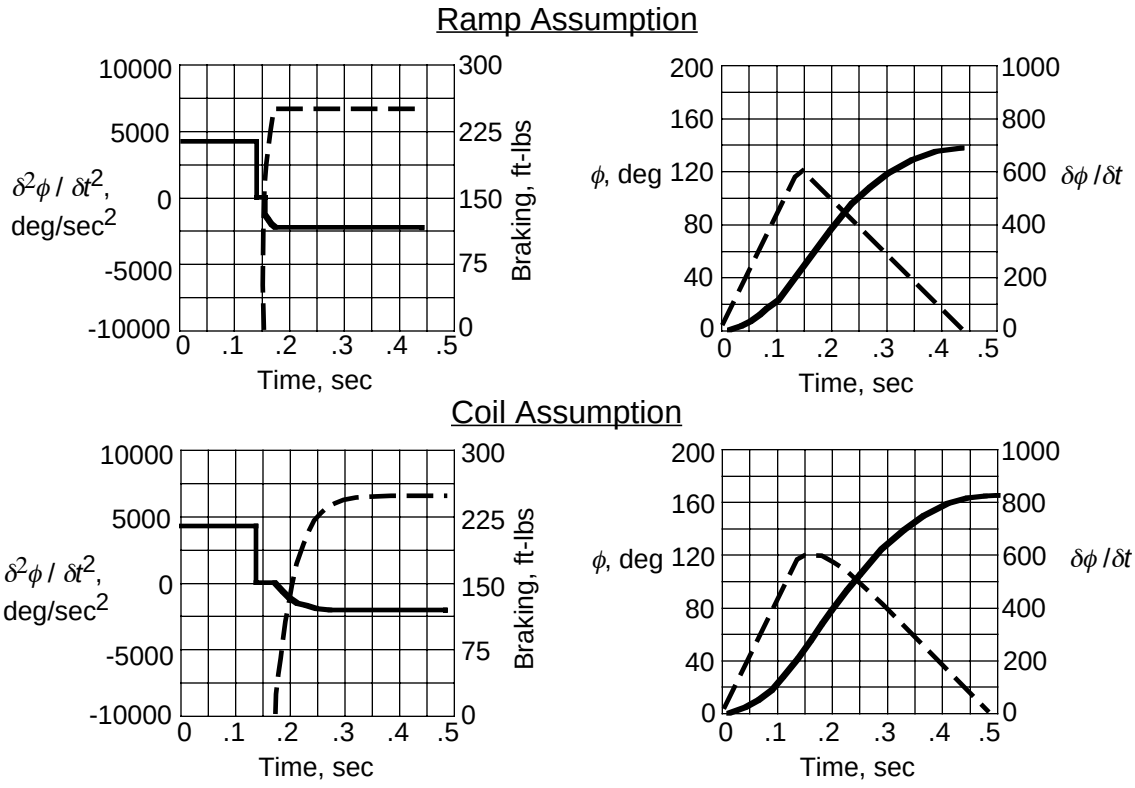

Figure 12. Typical brake performance.

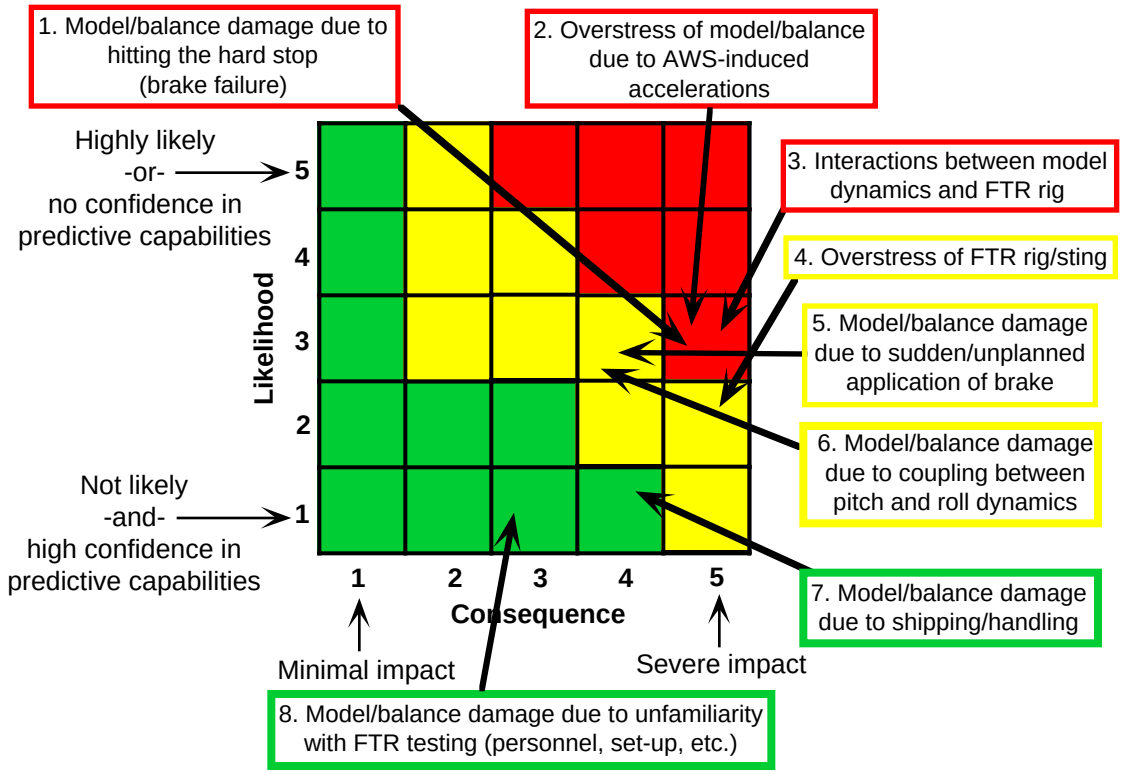

Figure 13. Initial risk assessment.

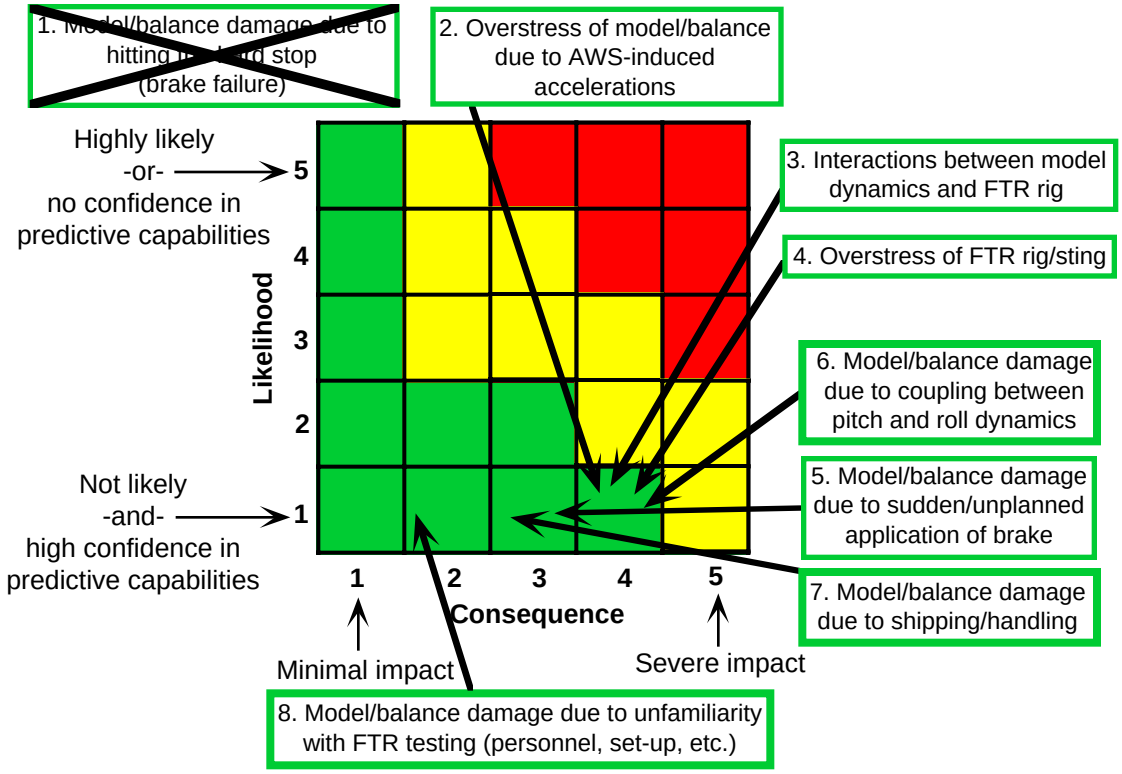

Figure 14. Risk assessment after risk mitigations.

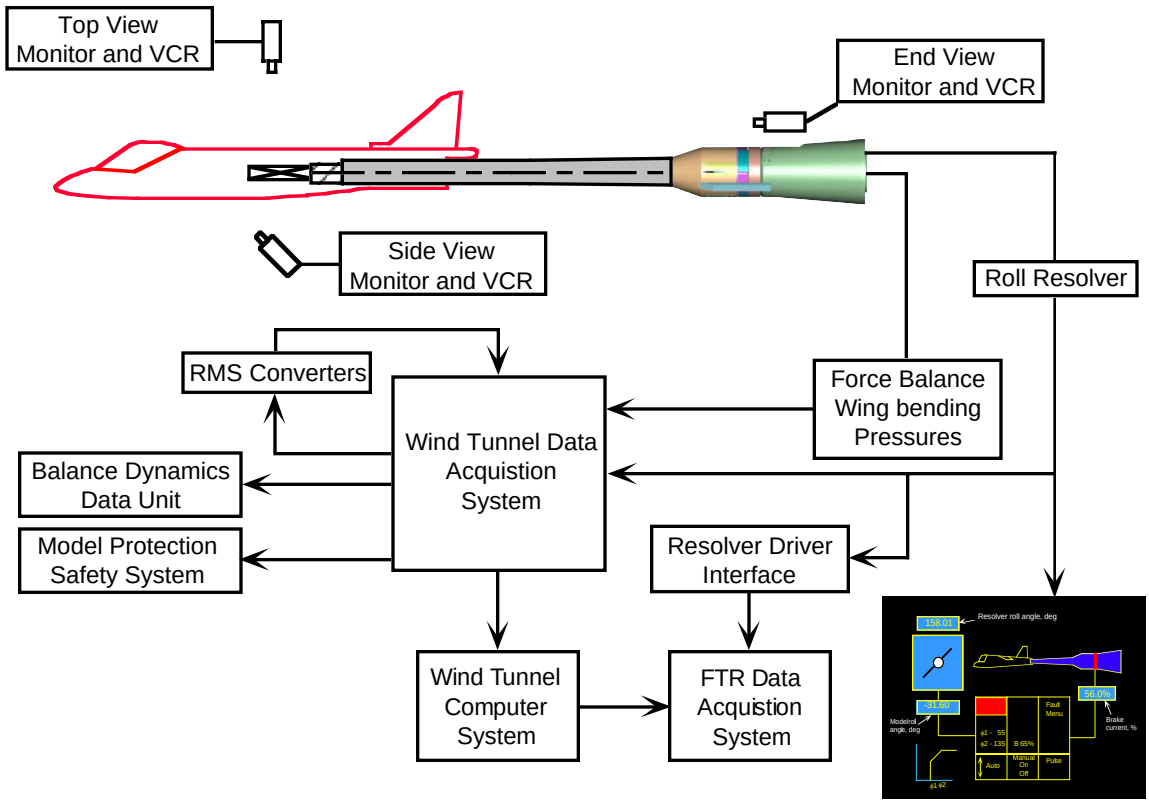

Figure 15. Schematic of experimental setup

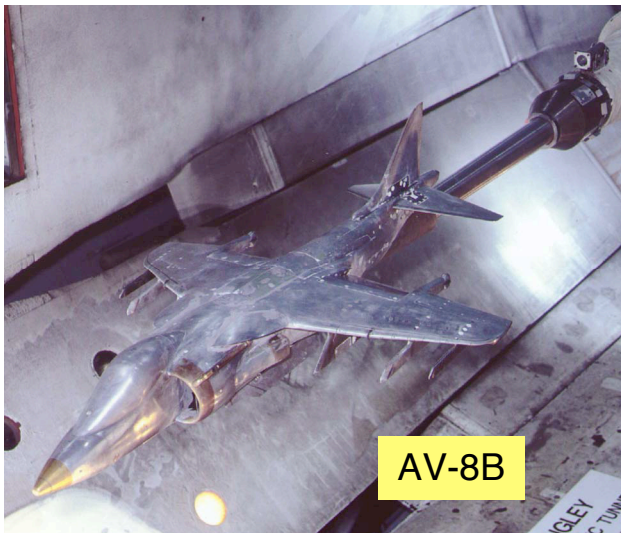

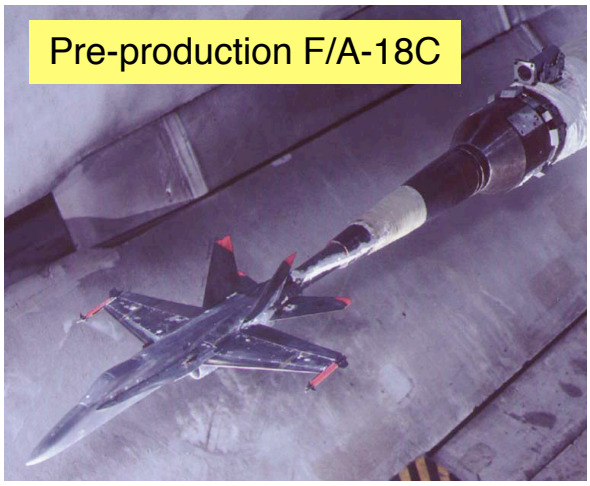

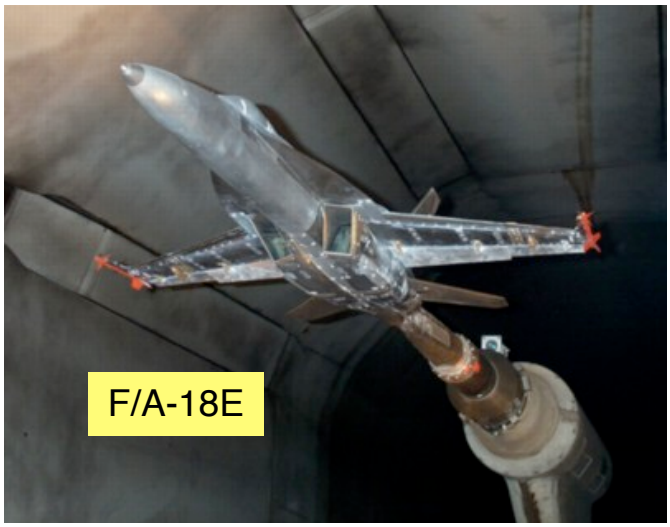

Figure 16. Photographs of the models tested.